

NRQCD Results on Form Factors*

S. Hashimoto^a, K. Ishikawa^b, H. Matsufuru^b, T. Onogi^b and N. Yamada^b

^a High Energy Accelerator Research Organization (KEK), Tsukuba 305, JAPAN

^b Department of Physics, Hiroshima University, 1-3-1 Kagamiyama, Higashi-Hiroshima 739, JAPAN

We report results on f_B and semi-leptonic B decay form factors using NRQCD. We investigate $1/M$ scaling behavior of decay amplitudes. For f_B Effect of higher order relativistic correction terms are also studied.

1. Introduction

Weak matrix elements of B meson such as f_B , B_B , and $B \rightarrow \pi(\rho)l\nu$ form factors are important quantities for the determination of Cabbibo-Kobayashi-Maskawa matrix elements. However simulating the b -quark with high precision is still a challenge in Lattice QCD, since the b -quark mass in the lattice unit is large, $am_b \sim 2-3$, even in recent lattice calculations. One approach to deal with the heavy quark is to extrapolate the matrix elements for heavy-light meson around the charm quark mass region to the b -quark mass assuming $1/m$ scaling. It is, however, rather difficult to control the systematic uncertainty in this approach, since the systematic error tends to become larger as increasing am_Q . An alternative approach is to use an effective nonrelativistic action. In Table 1, we compare various features of NRQCD[1], Fermilab[2], and ordinary Wilson/Clover actions as b -quark action. The first two actions are the effective nonrelativistic actions. Their advantage is that b -quark can be directly simulated.

In this report, we present our study of the decay constant of B meson and $B \rightarrow \pi l \bar{\nu}$ semi-leptonic decay form factors with NRQCD action. We study the mass dependence of these quantities by simulating heavy-light mesons over a wide range of the heavy quark mass. In section 2, we study the $1/m$ dependence of the heavy-light decay constant using nonrelativistic action of $O(1/m_Q^2)$. The systematic errors due the truncation of higher order relativistic correction terms

Table 1

Fermion actions for heavy quark.

NRQCD	Fermilab	Wilson/Clover
Direct Simulation	Direct Simulation	Extrapolation from charm
Error size $\frac{\alpha_s \Lambda}{m_Q}, \frac{\Lambda^2}{m_Q^2}$	Error size $\frac{\alpha_s \Lambda}{m_Q}, \frac{\Lambda^2}{m_Q^2}$	Error size $(am_Q)^2, \alpha_s am_Q$
Error remains as $\beta \nearrow$	Error $\rightarrow 0$ as $\beta \nearrow$	Error $\rightarrow 0$ as $\beta \nearrow$
Easily Improvable	Improvable	

are estimated. In section 3 we describe the first computation of the $B \rightarrow \pi l \bar{\nu}$ semi-leptonic decay form factors with NRQCD action of $O(1/m_Q)$. Section 4 is devoted for discussion and future problems.

2. B meson decay constant f_B

In the NRQCD approach it is very important to investigate the size of the systematic error arising from the truncation of the action at a certain order of $1/m_Q$. Earlier studies on f_B by Davies et al.[3] and Hashimoto[4] and the subsequent work by NRQCD group[5], where b -quark is simulated with the NRQCD action including up to $O(1/m_Q)$ terms, showed that $1/m_P$ correction of f_B from the static limit is significantly large. Thus the effect of the higher order correction of $O(1/m_Q^2)$ could be important. In this section, we compare the B meson decay constant obtained from the action including $O(1/m)$ terms only and that including $O(1/m^2)$ terms entirely.

*Talk presented at the International workshop "Lattice QCD on Parallel Computers", March 1997, Tsukuba

2.1. NRQCD action and field rotation

We employ the following NRQCD action

$$\begin{aligned}
S &= Q^\dagger(t, \mathbf{x}) \left[Q(t, \mathbf{x}) - \left(1 - \frac{aH_0}{2n}\right)^n \right. \\
&\quad \times \left(1 - \frac{a\delta H}{2}\right) U_4^\dagger \left(1 - \frac{a\delta H}{2}\right) \\
&\quad \left. \times \left(1 - \frac{aH_0}{2n}\right)^n Q(t-1, \mathbf{x}) \right] \quad (1)
\end{aligned}$$

where

$$H_0 = -\frac{\Delta^{(2)}}{2m_Q}, \quad (2)$$

$$\delta H = \sum_i c_i \delta H^{(i)}, \quad (3)$$

$$\delta H^{(1)} = -\frac{g}{2m_Q} \boldsymbol{\sigma} \cdot \mathbf{B}, \quad (4)$$

$$\delta H^{(2)} = \frac{ig}{8m_Q^2} (\boldsymbol{\Delta} \cdot \mathbf{E} - \mathbf{E} \cdot \boldsymbol{\Delta}), \quad (5)$$

$$\delta H^{(3)} = -\frac{g}{8m_Q^2} \boldsymbol{\sigma} \cdot (\boldsymbol{\Delta} \times \mathbf{E} - \mathbf{E} \times \boldsymbol{\Delta}), \quad (6)$$

$$\delta H^{(4)} = -\frac{(\Delta^{(2)})^2}{8m_Q^3}, \quad (7)$$

$$\delta H^{(5)} = \frac{a^2 \Delta^{(4)}}{24m_Q}, \quad (8)$$

$$\delta H^{(6)} = -\frac{a(\Delta^{(2)})^2}{16nm_Q^2}, \quad (9)$$

where n denotes the stabilization parameter. The coefficients c_i are unity at tree level and should be determined by perturbatively matching the action to that in relativistic QCD in order to include the 1-loop corrections. Δ and $\Delta^{(2)}$ denote the symmetric lattice differentiation in spatial directions and Laplacian respectively and $\Delta^{(4)} \equiv \sum_i (\Delta_i^{(2)})^2$. \mathbf{B} and \mathbf{E} are generated from the standard clover-leaf field strength.

The original 4-component heavy quark spinor h is decomposed into two 2-component spinors Q and χ after Foldy-Wouthuysen-Tani (FWT) transformation:

$$h(x) = R \begin{pmatrix} Q(x) \\ \chi^\dagger(x) \end{pmatrix}, \quad (10)$$

where R is an inverse FWT transformation matrix which has 4×4 spin and 3×3 color indices.

After discretization, at the tree level R is written as follows:

$$R = \sum_i R^{(i)}, \quad (11)$$

$$R^{(1)} = 1, \quad (12)$$

$$R^{(2)} = -\frac{\boldsymbol{\gamma} \cdot \boldsymbol{\Delta}}{2m_Q}, \quad (13)$$

$$R^{(3)} = \frac{\Delta^{(2)}}{8m_Q^2}, \quad (14)$$

$$R^{(4)} = \frac{g\boldsymbol{\Sigma} \cdot \mathbf{B}}{8m_Q^2}, \quad (15)$$

$$R^{(5)} = -\frac{ig\gamma_4 \boldsymbol{\gamma} \cdot \mathbf{E}}{4m_Q^2}, \quad (16)$$

where

$$\Sigma^j = \begin{pmatrix} \sigma^j & 0 \\ 0 & \sigma^j \end{pmatrix}. \quad (17)$$

We apply the tadpole improvement[7] to all link variables in the evolution equation and R by rescaling the link variables as $U_\mu \rightarrow U_\mu/u_0$.

We define two sets of action and current operator $\{\delta H, R\}$ as follows,

$$\text{setI} \equiv \{\delta H_I, R_I\} \quad \text{and} \quad \text{setII} \equiv \{\delta H_{II}, R_{II}\} \quad (18)$$

where

$$\delta H_I = \delta H^{(1)} \quad \text{and} \quad R_I = \sum_{i=1}^2 R^{(i)}, \quad (19)$$

$$\delta H_{II} = \sum_{i=1}^6 \delta H^{(i)} \quad \text{and} \quad R_{II} = \sum_{i=1}^5 R^{(i)}. \quad (20)$$

δH_1 and R_1 include only $O(1/m_Q)$ terms while δH_2 and R_2 keep entire $O(1/m_Q^2)$ terms and the leading relativistic correction to the dispersion relation, which is an $O(1/m_Q^3)$ term. The terms improving the discretization errors appearing in H_0 and time evolution are also included.

Using these two sets, we can realize two levels of accuracy of $O(1/m_Q)$ and $O(1/m_Q^2)$.

2.2. Simulation methods

We have computed f_B at $\beta = 5.8$ on $120 \times 16^3 \times 32$ lattices with periodic boundary condition in the spatial direction and Dirichlet boundary condition in the temporal direction. The inverse lattice spacing a^{-1} determined from m_ρ is 1.714(63)

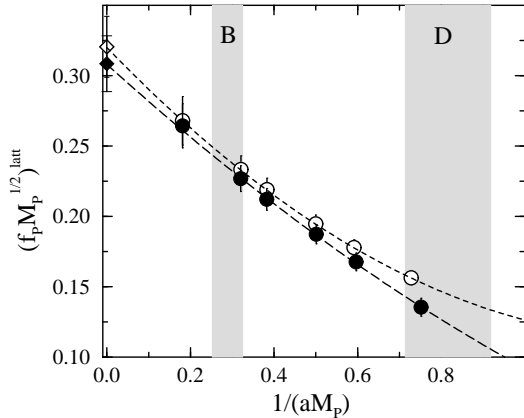


Figure 1. $1/M_P$ dependence of decay constant with the $O(1/m_Q)$ action (open circles) and the $O(1/m_Q^2)$ action (filled circles).

GeV. For heavy quark, we use both mean-field improved $O(1/m_Q)$ and $O(1/m_Q^2)$ NRQCD action. We take six points for the heavy quark mass am_Q in a range 0.9–5.0 (1.5–8.5 GeV). For light quark, we use Wilson action at $\kappa=0.1600, 0.1585,$ and 0.1570 ($k_{\text{crit}} = 0.16337$) which correspond to $m_s - 2m_s$.

2.3. Results

We show our results of $f_P\sqrt{m_P}$ in Figure 1. We find that the size of $O(1/m_P^2)$ correction is as small as about 3 % around the B meson region and about 15 % around the D meson region.

In order to see how the correction terms in the rotation of operator (13)–(16) changes the result, we show the contributions from each correction term to $f_P\sqrt{m_P}$ in Figure 2. We find that $O(1/m_Q)$ corrections are rather large. On the other hand, each of the three $O(1/m_Q^2)$ correction is about 2 % around the B meson region. There is a cancellation among the three corrections, and the total effect is of 3%. Although the effect of the higher order corrections is naively expected to be very small, there is no guarantee whether this cancellation takes place at higher order. We, therefore, estimate an upper bound for the $O(1/m_P^3)$ error to be of 6% at B meson region.

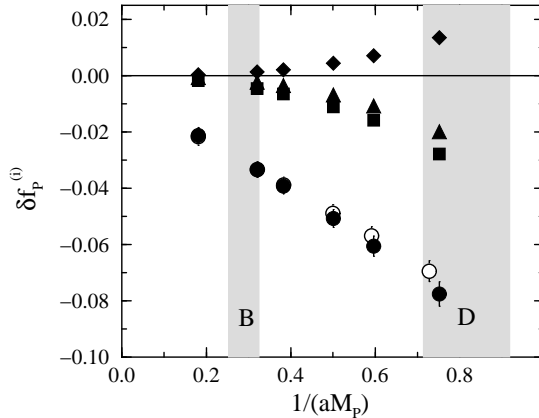


Figure 2. Corrections to the decay constant from each term of the current rotation. Circles represent the correction of $1/m_Q$ term (13) with $O(1/m_Q)$ (open circles) and $O(1/m_Q)^2$ (filled circles) actions. Squares, diamonds and triangles are corresponding to the corrections from $1/m_Q^2$ terms (14), (15), and (16) respectively.

We study $1/m_P$ dependence of $f_P\sqrt{m_P}$ by fitting the data with the following form

$$f_P\sqrt{m_P} = (f_P\sqrt{m_P})^\infty \left(1 + \frac{c_1}{m_P} + \frac{c_2}{m_P^2} + \dots\right),$$

for which we obtain

$$\begin{aligned} (f_P\sqrt{m_P})^\infty &= 0.308(20), \\ c_1 &= -0.87(11), \\ c_2 &= 0.17(11). \end{aligned}$$

with the entire $O(1/m_Q^2)$ calculation. In physical units $c_1 = -1.49(19)\text{GeV}, c_2 = (0.71(23)\text{GeV})^2$,

To summarize, our analysis of f_B shows that $O(1/m_Q^2)$ relativistic correction is of about 3 % and $1/m_P$ expansion from the static limit has a good behavior[8]. In order to obtain f_B with higher precision, one has to control other systematic errors such as perturbative and discretization errors. We have not included one-loop correction for the renormalization constant, for which the calculation is underway. NRQCD group recently calculated the full one-loop renormalization factor for the decay constant with nonrelativistic heavy quark of $O(1/m_Q)$ and clover light

quark[6]. They find that the effect of operator ∂P_5 which appear at one-loop level significantly reduces the decay constant. We are also planning to carry out the simulations at higher β values with $O(a)$ -improved Wilson light quark to remove $O(a)$ error in near future.

3. B meson semi-leptonic decay form factors

In this section we report our study of $B \rightarrow \pi l \bar{\nu}$ semi-leptonic decay form factors. This is the first calculation with the NRQCD action. Earlier attempts to calculate the form factors were made by APE[9], UKQCD[10], Wuppertal[11] by extrapolating the results in the D meson mass region obtained with the clover action assuming heavy quark scaling law. Direct simulation would be certainly necessary as an alternative approach just as in the calculation of f_B in order to investigate the mass dependence and to obtain reliable results. The status of form factors with Wilson/Clover as well as Fermilab action is summarized in refs.[12,13].

The semi-leptonic decay form factors f^+ and f^0 are defined as follows

$$\begin{aligned} & \langle \pi(k) | V_\mu | B(p) \rangle \\ &= \left(p + k - q \frac{m_B^2 - m_\pi^2}{q^2} \right)_\mu f^+(q^2) \\ & \quad + q_\mu \frac{m_B^2 - m_\pi^2}{q^2} f^0(q^2) \end{aligned} \quad (21)$$

where $q_\mu = p_\mu - k_\mu$ and $|B(p)\rangle$ has a normalization

$$\langle B(p) | B(p') \rangle = (2\pi)^3 2E_B(p) \delta^3(\mathbf{p} - \mathbf{p}'). \quad (22)$$

The virtual W boson mass q^2 takes a value in a region $0 \leq q^2 \leq q_{max}^2$ where $q_{max}^2 = (m_B - m_\pi)^2$. In the rest frame of the initial B meson, pion is also almost at rest in the large q^2 region ($q^2 \approx q_{max}^2$), where the W boson carries a large fraction of released energy from the B meson. In the small q^2 region ($q^2 \approx 0$), on the other hand, the pion is strongly kicked and has a large spatial momentum ($\mathbf{k}_\pi \sim$ a few GeV/c). Lattice calculation is not reliably applicable for the small q^2 region, since the discretization error of $O(a\mathbf{k}_\pi)$ becomes

unacceptably large. This leads to a fundamental restriction in the kinematical region where lattice calculation may offer a reliable result.

The differential decay rate is given as

$$\begin{aligned} & \frac{d\Gamma(\bar{B}^0 \rightarrow \pi^+ l^- \bar{\nu})}{dq^2} \\ &= \frac{G_F^2 |V_{ub}|^2}{192\pi^3 m_B^3} \lambda^{3/2}(q^2) |f^+(q^2)|^2 \end{aligned} \quad (23)$$

where

$$\lambda(q^2) = (m_B^2 + m_\pi^2 - q^2)^2 - 4m_B^2 m_\pi^2. \quad (24)$$

The decay rate vanishes at $q^2 = q_{max}^2$ because the phase space gets smaller. It is, thus, essential to calculate $f^+(q^2)$ in a q^2 region where the experimental data will become available and the systematic error does not spoil the reliability, in order to determine $|V_{ub}|$ model independently.

Another important feature of the B meson semi-leptonic decay is the implication of the Heavy Quark Effective Theory (HQET)[14]. In the heavy quark mass limit, it is more natural to normalize the heavy meson state as

$$\langle \tilde{M}(p) | \tilde{M}(p') \rangle = (2\pi)^3 2 \left(\frac{E_M(p)}{m_M} \right) \delta^3(\mathbf{p} - \mathbf{p}') \quad (25)$$

instead of the covariant normalization (22). With this normalization, the large mass scale m_M is removed from the theory and one can use the heavy quark expansion. The amplitude may be expanded as

$$\begin{aligned} & \langle \pi(k) | V_\mu | \tilde{M}(p) \rangle \\ &= \langle \pi(k) | V_\mu | M(p) \rangle / \sqrt{m_M} \\ &= X_\mu^\infty(v \cdot k) \\ & \quad \times \left(1 + \frac{c_1(v \cdot k)}{m_M} + \frac{c_2(v \cdot k)}{m_M^2} + \dots \right) \end{aligned} \quad (26)$$

where v is a velocity of the heavy meson and c_1, c_2, \dots are functions of $v \cdot k$. It is worth to note that the heavy quark mass extrapolation and interpolation have to be done with $v \cdot k$ fixed. In the rest frame of the heavy meson, this condition implies fixed pion momentum, since $v \cdot k$ becomes $\sqrt{m_\pi^2 + \mathbf{p}_\pi^2}$. We propose to study the $1/M$ dependence of the following quantities

$$V_4(k, p) \equiv \frac{\langle \pi(k) | V^4(0) | B(p) \rangle}{\sqrt{2E_\pi} \sqrt{2E_B}}, \quad (27)$$

$$V_k(k, p) \equiv \frac{\langle \pi(k) | \frac{1}{k^2} \sum_i k^i \cdot V^i(0) | B(p) \rangle}{\sqrt{2E_\pi} \sqrt{2E_B}}, \quad (28)$$

which are natural generalization of $f_P \sqrt{M_P}$ for the heavy-light decay constant. Indeed these quantities are almost raw number which one obtains in the lattice calculation as magnitudes of corresponding three-point functions, and then free from other ambiguities such as the choice of mass parameter of the heavy quark and the discretization of the spatial momenta.

3.1. NRQCD action and simulation parameters

The action we used for the semi-leptonic decay differs from that in the f_B calculation.

$$S = Q^\dagger(t, \mathbf{x}) \left[\left(1 - \frac{aH_0}{2n}\right)^{-n} U_4 \left(1 - \frac{aH_0}{2n}\right)^{-n} Q(t+1, \mathbf{x}) - (1 - a\delta H) Q(t, \mathbf{x}) \right], \quad (29)$$

where

$$H_0 = -\frac{\Delta^{(2)}}{2m_Q}, \quad (30)$$

$$\delta H = -\frac{g}{2m_Q} \boldsymbol{\sigma} \cdot \mathbf{B}. \quad (31)$$

Notation is the same as in section 2.1. The FWT transformation operator R is identical to that in eq. (19) Numerical simulation has been done on the same 120 gauge configurations as was used for the decay constant. For the light quarks we use the Wilson fermion at $\kappa = 0.1570$. The following six sets of parameters for the heavy quark mass and the stabilization parameter; $(m_Q, n) = (5.0, 1), (2.6, 1), (2.1, 1), (1.5, 2), (1.2, 2),$ and $(0.9, 2)$. $m_Q = 2.6$ and 0.9 roughly correspond to b - and c -quark masses respectively.

3.2. Extraction of three-point functions

Matrix elements are extracted from the three-point correlation functions:

$$C_\mu^{(3)}(\mathbf{k}, \mathbf{p}; t_B, t_V, t_\pi) = \sum_{x_f, x_s} e^{-ip \cdot x_B} e^{-i(k-p) \cdot x_V} \langle 0 | O_B(t_B, \mathbf{x}_B) V_\mu^\dagger(t_V, \mathbf{x}_V) O_\pi^\dagger(t_\pi, 0) | 0 \rangle$$

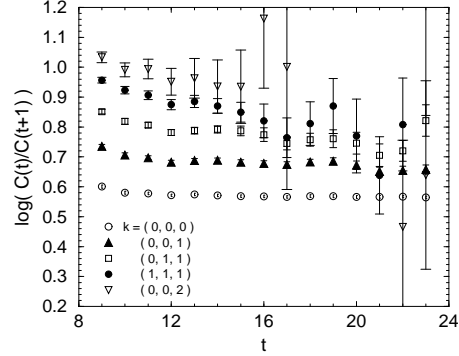


Figure 3. Effective mass plot for the pion with finite spatial momenta.

$$\begin{aligned} & \rightarrow \frac{Z_\pi(k) Z_B(p)}{2E_\pi(k) 2E_B(p)} \\ & \times e^{-E_\pi(k)(t_V - t_\pi)} e^{-E_B(p)(t_B - t_V)} \\ & \times \langle B(p) | V_\mu^\dagger | \pi(k) \rangle \\ & \quad (\text{for } t_B \gg t_V \gg t_\pi) \end{aligned} \quad (32)$$

where t_B , t_V and t_π indicate the location of the initial state B meson, heavy-light current and the final state pion respectively. We fix $t_\pi = 4$ and $t_V = 14$, and t_B is a variable. The amplitude $\langle \pi(k) | V_\mu | B(p) \rangle / \sqrt{2E_\pi} \sqrt{2E_B}$ is obtained by dividing the above expression by the corresponding two-point functions.

3.3. Effective masses

In this section, we present our numerical results.

In order to see whether the contamination from the excited state is sufficiently small, we examine the effective mass plots of the two-point functions of pion and B meson, and three-point functions.

Figure 3 shows the effective mass plot for the pion with finite spatial momenta up to $|\mathbf{a}\mathbf{k}| = 2(2\pi/16)$. Correlation functions seem to reach to the ground state beyond $t = 14$, except for $\mathbf{a}\mathbf{k} = (0, 0, 2)$ where statistical error becomes too large to extract reliable ground state energy. We, therefore, use momentum values up to $|\mathbf{a}\mathbf{k}| = \sqrt{3}(2\pi/16)$ in the following analysis. The

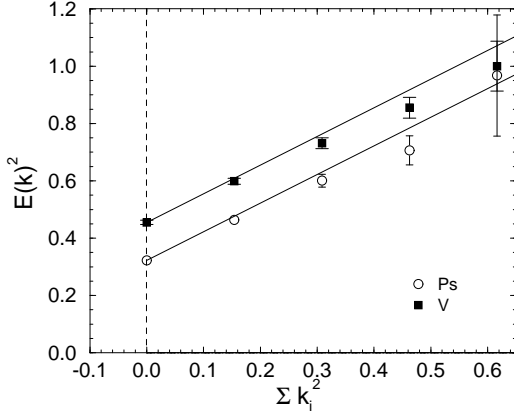


Figure 4. Dispersion relation for the π and ρ mesons at $\kappa = 0.1570$.

maximum momentum value corresponds to ~ 1 GeV/c in the physical unit.

The momentum dependence of the pion energy should obey the dispersion relation

$$E_{\pi}(\mathbf{k})^2 = m_{\pi}^2 + \mathbf{k}^2 \quad (33)$$

in the continuum limit. Then the deviation of the lattice dispersion relation from the continuum one is a good indicator of the discretization error. In figure 4 we plot the dispersion relation for π and ρ mesons measured in our simulations. Solid lines represent the above expression (33), which does not fit the measured point, showing the effect of the $O(a)$ discretization error.

A similar plot for the B meson is found in Figure 5, where the maximum momentum is $|\mathbf{k}| = \sqrt{3}(2\pi/16)$. The fitting interval is chosen to be 16-24 where the contamination of excited state is negligible for each momentum values.

Figures 6 and 7 show the effective mass plots for three point functions with temporal and spatial currents respectively. The location of the interpolating field of the B meson is varied to define the effective mass, then the energy should coincide with that obtained from the two-point function if the ground state is sufficiently isolated. We

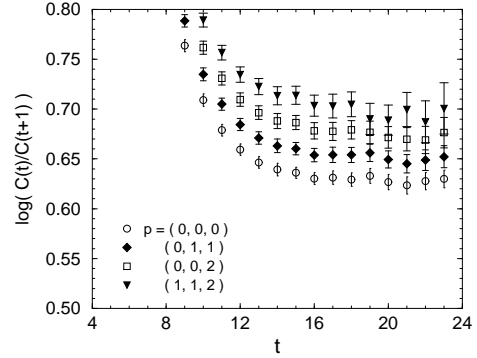


Figure 5. The effective plots for the heavy-light two-point function at $am_Q = 2.6$ and $\kappa = 0.1570$.

observe clear plateau in a wide range for t of 23-28 and the mass values consistent with that from the two-point functions, which are shown as solid lines in the figures.

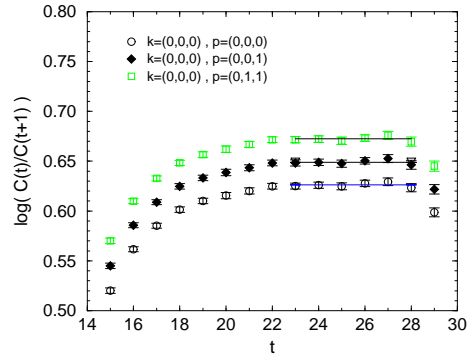


Figure 6. Effective mass plot for the three point function with the fourth component of the vector current V_4 .

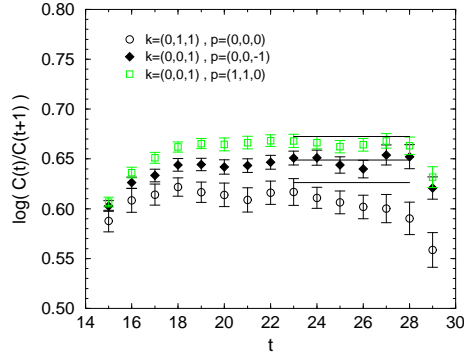


Figure 7. Effective mass plot for the three point function with the spatial component of the vector current V_i .

3.4. $1/m$ dependence

We are now confident that the ground state is reliably extracted for both two-point and three-point functions, and present the results for the matrix elements. Since $1/m$ dependence of the matrix elements is the main issue in this study, we plot V_4 and V_k , defined in (27) and (28) respectively, which obeys the simple heavy mass scaling law (26), in Figures 8 and 9. We observe that $1/m$ dependence of matrix elements is rather small in contrast to the large $1/m$ correction for the heavy-light decay constant $f_P\sqrt{m_P}$. Although intuitive interpretation of this result is difficult, the smallness of the $1/m$ correction is a good news to obtain the form factor with high precision, because the error in setting the b -quark mass does not affect the prediction. And also this behavior is consistent with the previous works[9,10,12,11], in which the heavy quark mass is much smaller than ours.

The q^2 dependence of the form factors f^+ and f^0 is shown in Figure 10. The heavy quark mass is roughly corresponding to the b -quark. As we discussed previously the accessible q^2 region is rather restricted. It is, however, interesting that already at this stage one is able to see the momentum dependence which could really be tested by looking

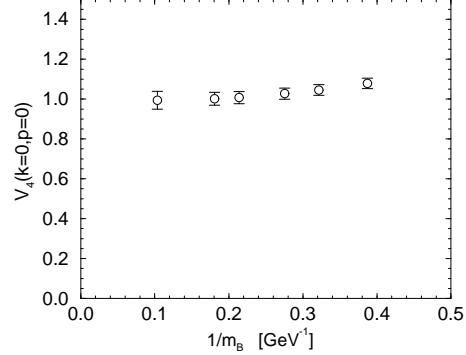


Figure 8. $1/m$ dependence of the matrix element V_4 in eq.(27) at zero recoil.

at the momentum spectrum data in the future B factories.

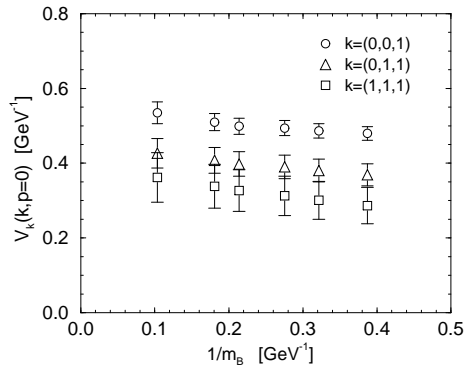


Figure 9. $1/M$ dependence of the matrix element V_k in eq. (28). Circles, diamonds and squares correspond to pion momenta $k=(0,0,1)$, $(0,1,1)$ and $(1,1,1)$ respectively.

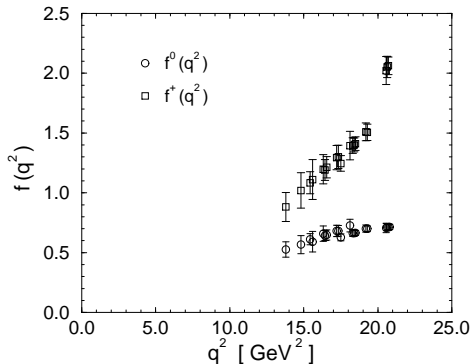


Figure 10. q^2 dependences of the form factors f^0 , f^+ .

4. Discussion

We have studied $1/m_Q$ dependence of the heavy-light decay constant and semi-leptonic decay form factors with NRQCD action. We find that the error of truncating higher order relativistic correction term is as small as 6% for the decay constant. We also find that the semi-leptonic decay form factor for $B \rightarrow \pi l \bar{\nu}$ has very small $1/m_Q$ dependence, which is consistent with the previous results in the Wilson/Clover approach.

To obtain the physical result for extracting V_{ub} matrix elements, chiral limit for the light quark must be taken and calculation of the renormalization constant Z_V at one-loop is required, which is now underway.

One of the largest problem is that so far, due to low statistics and the discretization errors of $O((a\mathbf{k})^2)$, lattice calculation works only for rather small recoil region, where the statistics of the experimental data is not high due to the phase space suppression. We are planning to carry out simulations with much higher statistics, with larger β and with improved light quarks so that we can push up the accessible momentum region. It is also true that more data from CLEO, or future B factories is required for relatively small recoil region $|\mathbf{k}_\pi| \sim 1$ GeV, where the lattice calculation

is most reliable.

5. Acknowledgment

Numerical calculations have been done on Paragon XP/S at INSAM (Institute for Numerical Simulations and Applied Mathematics) in Hiroshima University. We are grateful to S. Hioki for allowing us to use his program to generate gauge configurations. We would like to thank J. Shigemitsu, C.T.H. Davies, J. Sloan and the members of JLQCD collaboration for useful discussions. H.M. would like to thank the Japan Society for the Promotion of Science for Young Scientists for a research fellowship. S.H. is supported by Ministry of Education, Science and Culture under grant number 09740226. and the members of JLQCD collaboration for useful discussions. H.M. would like to thank the Japan Society for the Promotion of Science for Young Scientists for a research fellowship. S.H. is supported by Ministry of Education, Science and Culture under grant number 09740226.

REFERENCES

1. B. A. Thacker and G. P. Lepage, Phys. Rev. **D43**, 196 (1991); G.P. Lepage, L. Magnea, C. Nakhleh, U. Magnea and K. Hornbostel, Phys. Rev. **D46** 4052 (1992).
2. A.X. El-Khadra, A.S. Kronfeld and P.B. Mackenzie, Phys. Rev. **D55** (1997) 3933.
3. UKQCD Collaboration, presented by C. T. H. Davies, Nucl. Phys. B (Proc. Suppl.) **30**, 437 (1993).
4. S. Hashimoto, Phys. Rev. **D50**, 4639 (1994).
5. A. Ali Khan *et al.*, Nucl. Phys. B(Proc. Suppl.)**47**, 425 (1996); S. Collins *et al.*, Phys. Rev. **D55**, 1630 (1997); A. Ali Khan *et al.*, hep-lat/9704008.
6. J. Shigemitsu, hep-lat/9705017.
7. G.P. Lepage and P.B. Mackenzie, Phys. Rev. **D48**(1993)2250.
8. K. Ishikawa, H.Matsufuru, T. Onogi, N. Yamada and S. Hashimoto hep-lat/9706008.
9. A. Abada *et al.*, Phys. Lett. **B365**, 275 (1996), C.R.Allton *et al.*, Phys. Lett. **B345**,

- 513 (1995), A. Abada et al., Nucl. Phys. **B416**, 675 (1994).
10. UKQCD collaboration, D.R. Burford et al., Nucl. Phys. **B447**, 425 (1995).
 11. G. Gusken, K. Schilling and G. Siegert, Nucl. Phys. B (Proc. Suppl.) **47**, 485 (1996).
 12. J.Simone, Nucl. Phys. B (Proc. Suppl.) **47**, 17 (1996).
 13. J.Flynn, Nucl. Phys. B (Proc. Suppl.) **53**, 168 (1997).
 14. For a review see, e.g. M. Neubert, Phys. Rep. **245**, 259 (1994).